Comparing Flow-Reversal and Inner Recirculation Reactors: Experiments and Simulations

Moshe Ben-Tullilah, Einat Alajem, Rina Gal and Moshe Sheintuch
Dept. of Chemical Engineering, Technion, Haifa, Israel 32000

The operation of reactors with flow reversal operate similar to a reactor with internal recirculation, which the feed enters through one (say, inner) reactor and then turns around and flows out through (the outer) another, when the heat-transfer coefficient between the tubes is large. In this study, we compare the behavior of a packed-bed reactor operating in flow-reversal or internal-recirculation modes, using ethylene oxidation on Pt/Al_2O_3 as a model reaction. The reactor was built from two concentric tubes (with 28.5 and 42.5 mm in diameter), both packed with a 20 cm catalytic bed and 10 cm inert beds (of alumina-pellets) on each side. An adjustable opening between the tubes allowed for an internal recycle mode and the whole system could be operated with periodic flow reversal. The reactor can be employed then either as a simple once-through bed or as a bed with flow reversal in the inner tube or as bed with internal recirculation flowing from the inner to outer tube, or in the opposite direction, as well as an internal-recirculation reactor with flow reversal. Due to heat losses, the latter two modes were inferior to the others. The experiments, backed by simulations using a homogeneous model with independently determined parameters, showed that the technically-simpler inner-outer internal-recycle reactor operated better at low flow rates, than that with flow reversal, but the conclusion is reversed at high flow rates. The domain where the internal-recirculation reactor is superior depends on the heat-transfer coefficient between the streams. By lowering the feed concentration, the extinction point was determined for each mode highlighting again the conclusions drawn above that inner-recirculation operation may be superior to flow reversal at low flow rates. Simulations revealed also the existence of solutions with stationary fronts or oscillatory fronts.

Introduction

Reactors with flow reversal have been a subject of intensive investigation in the past several years (Boreskov et al., 1979; Eigenberger and Nieken, 1988; Boreskov and Matros, 1983; Matros, 1989). This type of operation is similar under certain assumptions (see below) to that of two heat-exchanging reactors with counter-current flow. The latter is similar to a reactor with internal recirculation, in which the feed enters through one (say, inner) reactor and then turns around and flows out through another (the outer). If you attach two such mirror-imaged reactors, you will find an arrangement similar to the heat-exchanging reactor with countercurrent flow. Both types of operation depend on the heat-exchange coefficient and, although they are much simpler to operate, it has been claimed that, for practical values of coefficients, the performance of the flow-reversal reactor is superior to the other two. In the limit of infinitely-fast heat transfer the models of both reactors are similar to that of the flow-reversal reactor with fast switching of flow.

In this study we compare the behavior of a packed-bed reactor operating in flow-reversal or internal-recirculation modes, using ethylene oxidation on Pt/Al_2O_3 as a model reaction. The motivation of our work is the need to compare various direct or indirect modes of heat exchange. A reactor

Correspondence concerning this article should be addressed to.

with indirect heat-exchange can be arranged in various ways. Autothermal reactors, in which the feed is heated-up on the shell side before turning around and reacting in the catalyst side, have been employed for many years now (Froment and Bischoff, 1990). We employ here a tube-and-shell reactor with inner recirculation, where both sides are packed with a catalyst, so that the feed heats up and starts to react on the tube side before turning into the shell side. In a commercial operation we envision the two reactors organized in a packed multitube arrangement within a shell that is packed as well. We can operate this reactor in one of several modes: as a once-through simple packed bed, as a flow-reversal reactor with flow in the inner tube, as an internal-recirculation reactor with flow entering the inner-tube or the outer-tube, and as an internal recirculation reactor with flow-reversal. The latter mode of operation combines the benefits of direct and indirect heat-transfer modes.

We are also interested in the dynamic behavior of such a unit and show that oscillatory behavior may emerge under certain time-independent conditions with simple kinetics. Recent studies that employed a packed bed in the form of a loop, with cocurrent flow on both sides of the reactor-heat-exchanger, led to surprisingly interesting oscillatory dynamics, even with simple kinetics; the oscillatory behavior emerged due to thermal effects and the feedback of traveling fronts (Lauschke and Gilles, 1994). The dynamics of a fixed bed with an external recycle have been analyzed extensively (Burghardt et al., 1999).

We compare experimental observations during ethylene oxidation on Pt/Al_2O_3, with simulations of this reactor using a kinetic rate expression that was derived elsewhere. The oxidation of ethylene on supported Pt catalysts is a complex reaction characterized by self-inhibition due to high concentration of either ethylene and oxygen (expressed by Langmuir-Hinshelwood kinetics), by strong activation energy and by strong thermal effects that lead to a wide domain of steady-state multiplicity (Harmsen et al., 2000). This work complements our previous one on flow rate effects in flow-reversal reactors and the justification for the employed rate expression and its parameters are argued there (Ben-Tullilah et al., 2003). The experimental systems are similar to those in the previous study, but the reactors are different. This system suffers from heat-loss that distorts the results and the comparison.

Experimental System

The ethylene and air feedstreams (both of 99.9% purity) were supplied from cylinders and controlled by flowmeters (Brook Ltd.) before mixing. The air stream was passed through beds of silica-gel and activated carbon, to remove traces of water and organics, respectively (Figure 1).

The reactor, built in our machine-shop, consists of two concentric tubes (stainless-steel (316) tubes, with 28.5 and 47.2 mm in inner diameter and 0.5 and 1 mm wall-thickness, respectively), both packed with a 20-cm catalytic section between two 10-cm inert sections on each side. An adjustable position of the inner tube allowed to open or close a gate between the tubes; with the gate closed, the reactor operated only in the inner-tube while an open gate allowed for the internal recirculation mode. The whole system could be operated with periodic flow-reversal by means of a network of solenoid valves.

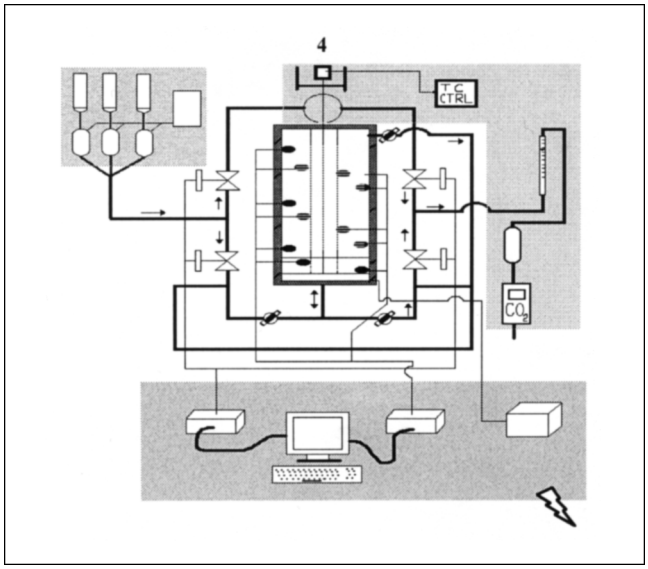

Figure 1. The experimental setup.

(1) Feed system; (2) Flow control; (3 and 4) step-up motor control of the sliding thermocouple position; (5) CO_2 analyzer; (6) computer control of the system; (7) data acquisition; (8) external heater control.

The reactor can be employed then in one of several modes (Figure 2):

(a) As a simple once-through bed in the inner tube, the outer tube is inactive then and acts as another insulation layer.

(b) As a bed with flow reversal in the inner tube.

(c) As a bed with inner recirculation with flow from the inner to the outer tube or in the opposite direction.

(d) As an inner-recirculation reactor with flow reversal.

Mode selection was determined by setting the corresponding computer-controlled solenoid valves and by adjusting the gate for internal recycle (see Figure 1).

Both reactor tubes were packed with a 0.5% Pt/Al_2O_3 catalyst (PMC Ltd.), with porosity of 0.4 and surface area of 365 m^2/g, in the form of spherical (1.6 mm in dia.) pellets. The inert sections were packed with inert alumina pellets. The catalyst was pretreated *in situ* to remove any adsorbed matter by heating it up in air at 460°K for 15 h followed by heating at 560°K for 12 h.

The reactor was heated resistively through a coiled wire wrapped around it. The reactor was covered with a 125 mm layer of glass-wool for insulation which in turn was wrapped with teflon tapes. The reactor temperature at the center was monitored with a sliding thermocouple (type K), moving through a capillary thermowall tube (1/16 in.). The thermocouple was controlled by a stepping motor. The wall temperature was monitored at 11 points by type K thermocouples placed 2.5 mm from the wall and 2.5 cm apart in the catalytic zone or 4.2 cm apart in the inert zone; their angular position was varied along an imaginary helix. The sliding thermocouple was designed to stop at locations opposite the fixed wall thermocouple. Data acquisition was performed by a PC 486 computer.

Gas composition was determined on-line and continuously with a CO_2 IR-analyzer, and off-line at desired times with a

(Perkin-Elmer) GC. The conversion determined from the (IR analyzed) CO_2 concentration were usually in some disagreement with those determined from (the GC analyzed) ethylene concentration; these differences were attributed to the CO_2 absorption capacity of the catalyst, as will be explained elsewhere.

The whole system was computer-controlled. At the start of each experiment, the data for the flow-controllers and solenoid valves were keyed into the control computer and the heating was applied to the reactor (when necessary) at a preset voltage under flow of air. Once the desired temperature has been reached, the ethylene was added and the desired parameters, like flow rates, cycle-period, or feed-composition, were changed automatically according to the preplanned experiment.

Experimental Results

Heat loss cannot be ignored in this relatively small experimental reactor, and we divide the description into two regimes: at high flow rates, the heat-production rate was sufficient to sustain the reactor even without external heating. At low flow rates (typically below 1 L/min), the heating element was operated in most runs in order to sustain an ignited state. The various modes are compared by noting the attainable temperature under similar heating powers and by determining the extinction point, upon declining feed concentration.

(a) No external heating

The heat production rate increased with flow rate and a family of profiles, measured in the inner reactor at different flow rates during internal-recirculation operation (Figure 3), exhibit a sharp jump at the entrance to the catalytic section, followed by a decline towards the exit. The maximal temperature increases linearly with flow rate (Figure 4). A typical profile in the inner and outer reactors, with feed from the inner reactor, is shown in Figure 5(a), and is compared with two other modes of operations: Internal-recirculation with flow entering at the outer tube leads to lower temperatures due to heat loss (Figure 5b). Periodic flow-reversal alternating between feed through the inner and through the outer tube leads to high temperatures in the half-cycle when feeding through the inner tube and low temperatures when the feed enters the outer reactor (Figure 5c).

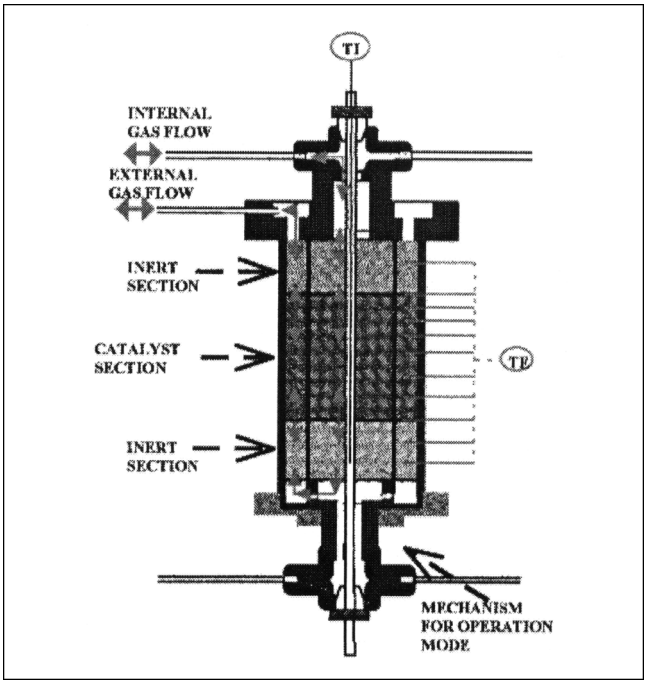

Figure 2. Structure of the reactor showing the feeds, catalytic and inert sections, sliding and fixed thermocouples, and passage that can be opened to operate in the recirculation mode.

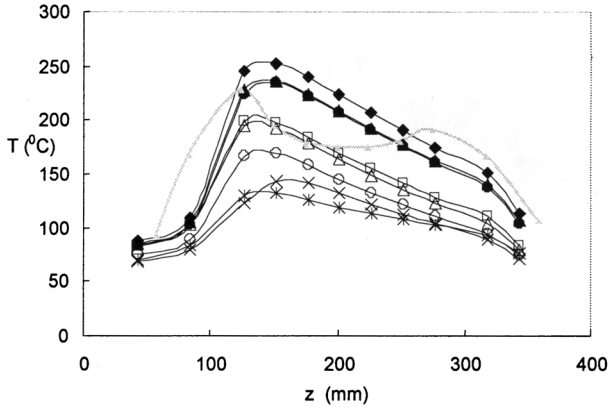

Figure 3. Experimental axial temperature profiles for inner recirculation mode (inner tube feeding) with various flow rates for ethylene feed concentration of 0.25%.

Results are compared with the profile flow reversal in the same concentration (double peak light line, after Ben-Tullilah et al. (2003).

Comparison of the internal-recirculation operation (Figure 3) with flow-reversal operation at similar conditions (0.25% ethylene in feed and flow rate of 10 L/min., see (Ben-Tullilah et al., 2003) shows that the hottest temperatures of the latter is lower, in spite of the higher flow rate.

With decreasing feed concentrations, at fixed flow rates to the internal-recirculation reactor, and at low flow rates, the front at the entrance shifts inwards, the peak temperature declines and, eventually, upon transition from 0.34 to 0.28%, the reactor extinguishes (Figure 6).

(b) Systems with External Heating

Recall that, at low flow rates, we had to operate the reactor with a certain external heating. In the absence of reaction the heated reactor exhibits a slightly parabolic and somewhat asymmetric profile due to heat loss at the edges in most runs. The average temperature was controlled by setting the voltage across the heating element. Within the catalytic section, the center temperature varied by few (about 5°) centigrade. The reactor temperatures in the absence of ethylene feed are reported below in all experiments. Most runs were conducted with feed flow rate of 500 cm^3/min; in several runs, we varied the flow rate.

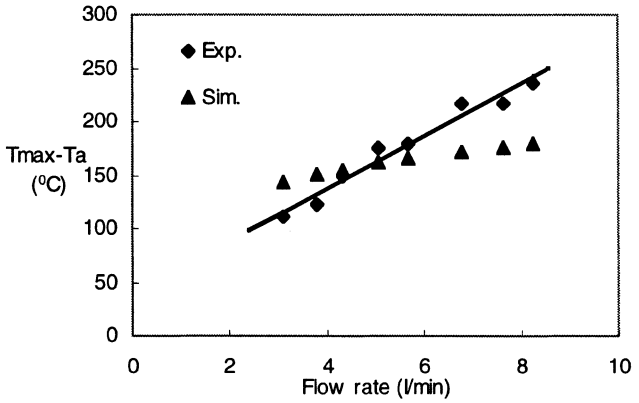

Figure 4. Experimental and simulated maximal temperature as a function of flow rate for the inner recirculation operation for feed concentration of 0.25%.

The simulated values were obtained with an A value that is twice that denoted in the Notation as the denoted value yielded extinguished states only.

(i) Flow-Reversal in the Inner Tube

We present below the dynamics of a single cycle after a periodic solution has been achieved, and the effect of feed concentration, cycle period, and flow rate on the periodic solution.

A typical dynamic pattern of a single (30-min) periodic flow-reversal cycle (Figure 7a) shows profiles at 7, 13, 20, and 26 min. It exhibits motion of the hot spot downstream (the feed initially is from the top or the right side of figure), along with a certain descend of the amplitude as the hot spot moves. As the feed position is switched to the bottom (or left side), the hot spot is established there and again moves downstream.

At high feed concentrations and high wall-temperatures (not shown), a double-peak profile is obtained, but, with declining concentration, the peaks temperatures decline and they coalesce eventually into a single-peak of larger amplitude. The effect of decreasing concentration is presented in Figure 8a. Eventually, the reactor is extinguished upon declining feed from 0.34 to 0.28% and stays so as the feed is decreased to 0.15%; increasing the feed concentration back to 0.43% did not lead to ignition of the reactor.

Increasing the feed flow rate at fixed feed concentration led, for the parameters specified, to increasing temperatures, to sharper peaks, and to a transition from a single- to double-peak structure with the peaks approaching the feed ports (Figure 9). While the apparent conversion declined somewhat, the maximal temperature and the average rate increases almost linearly with the flow rate (from 0.019 mole/min·g at 164 cc/min to 0.05 at 482 and 0.079 at 907 cc/min).

(ii) Internal-Recirculation Operation

Figure 7b presents the profiles along the inner and outer tubes, for recirculation-flow that is fed either through the inner or the outer tube. With flow into the inner tube, the reactor exhibits a sharp peak near the inlet and declining temperature downstream in the inner tube; then, the flow exits the inner-tube, turns around, and enters into the outer tube where it exhibits a similar, yet much cooler, profile. Under these conditions, and in the absence of reaction, the bed temperature is about 60°C. The temperatures are much smaller with recirculation flow entering the outer tube before turning into the inner one (Figure 7b), due to the strong heat loss from the outer tube.

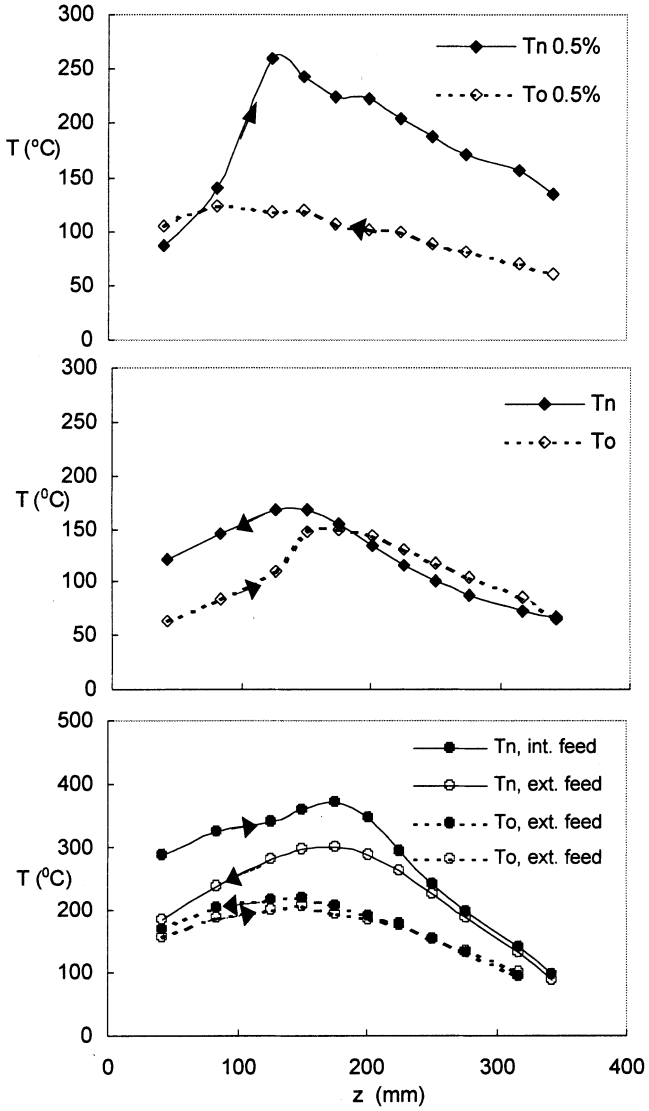

Figure 5. Experimental axial temperature profiles in the inner and outer reactors for three modes of operation.

Inner recirculation with flow entering at the inner tube (a) or the outer tube (b) and periodic flow reversal alternating between feed through the inner and outer tubes (c); flow rate of 5.7 L/min and feed concentration of 0.5%.

With declining feed concentration, and with feeding to the inner tube, the temperatures decline with a slight shift in the hot-spot position; the extinction point lies below 0.15% ethylene and could not be determined accurately (Figure 8b).

Comparison of the flow-reversal modes described above with the internal-recirculation mode shows that, at low flow rates and with comparable wall temperatures, the latter mode

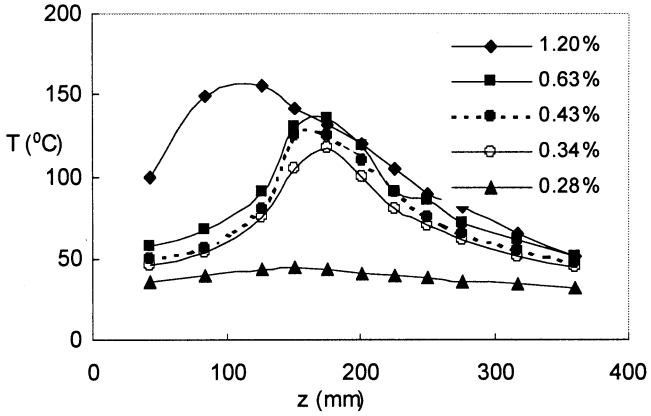

Figure 6. Experimental axial temperature profiles for recirculation operation (inner tube feeding) with various feed concentrations at a fixed flow rate of 0.5 L/min.

achieves higher temperatures everywhere (Figures 7 and 8) and a lower extinction point upon decreasing feed concentration (Figures 8 and 10) than the former. Peak temperatures of both modes are higher than those in the once-through operation (Figure 10).

When operated without external heating, and at low flow rates, the simple inner-outer internal-recirculation reactor exhibits higher temperature rises than those with flow reversal, and much better than those in the outer-inner reactor (not shown). By lowering the feed concentration, we determined the extinction point for each mode highlighting again the conclusions drawn above. This conclusion is later backed by simulations.

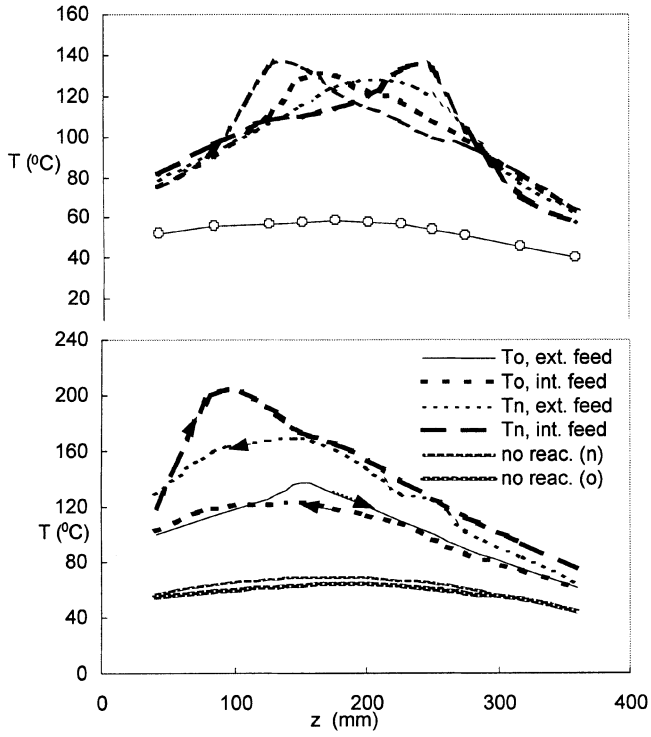

Figure 7. (a) Dynamic pattern of periodic flow reversal operation and (b) axial temperature profiles for recirculation flow with feed entering at the inner or outer tube for a flow rate of 0.5 L/min and a feed concentration of 0.9%.

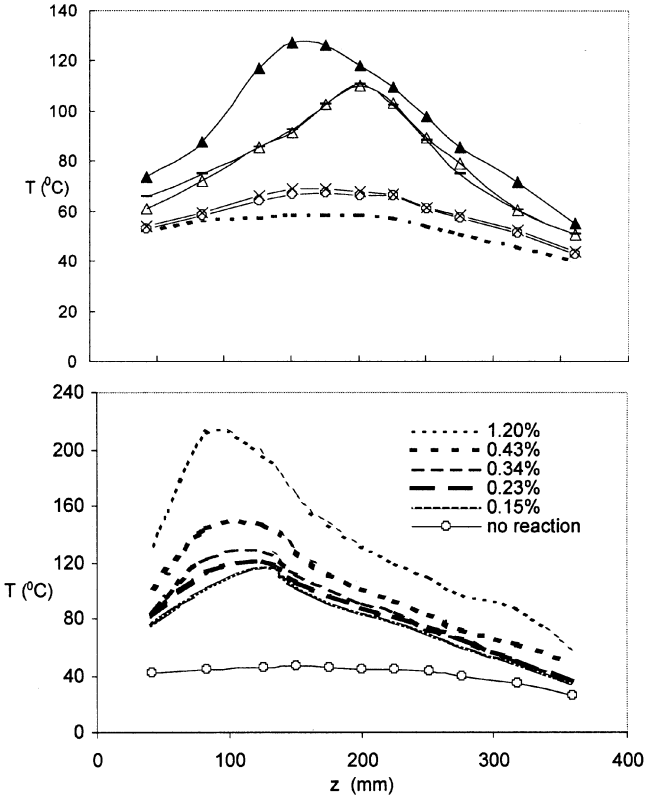

Figure 8. (a) Experimental axial temperature profiles for flow reversal operation and (b) inner recirculation with various ethylene feed concentrations for flow rate of 0.5 L/min.

The temperature in the absence of reaction is denoted.

Simulations

All of the results were simulated with a standard homogeneous model that accounts for convection, heat conduction, and axial dispersion. Except for the flow geometry, this model is similar to the extensively-studied models of the flow reversal reactors (Eigenberger and Nieken, 1988; Gawdzik and Rakowski, 1988; Thullie and Burghardt, 1990; Bhatia, 1991; Van de Beld and Westerterp, 1994; Rehacek et al., 1998). In our previous study of the flow-reversal operation, we did not find significant differences between the heterogeneous and homogeneous models, and we limit our simulations to the homogeneous model.

We consider now an internal recirculation reactor with once-through flow. The flow is fed from the left into the inner tube (denoted by superscript n), which has three zones (inert, catalytic, and inert) before turning around and feeding the outside tube (superscript o), which has the same three zones. Consider a catalytic packed bed of length L ($0 < z < L$), in which a reaction of general kinetics occurs (r is the rate of reaction), as well as heat loss at a rate UA_v. The heat and

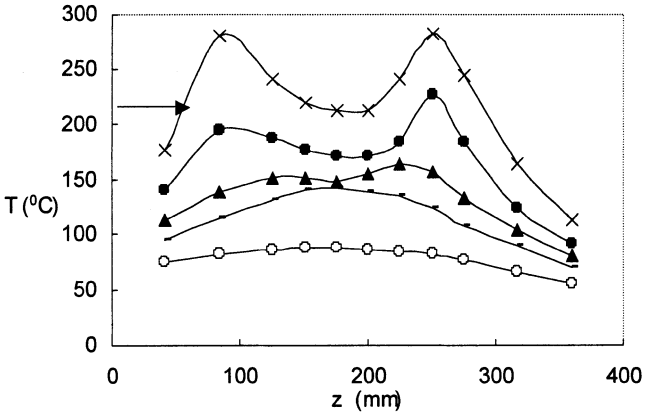

Figure 9. Experimental axial temperature profiles for flow reversal operation with various flow rates for feed concentration of 1.2%.

The temperature in the absence of reaction is denoted.

mass balances, in the inner and outer tube, are

$$\rho C_{P_{\text{eff}}} T_t^n - kT_{zz}^n + G^n C_{Pf} T_z^n = (-\Delta H)\rho r - (UA_V)^n (T^n - T^o) \quad (1)$$

$$\rho C_{P_{\text{eff}}} T_t^o - kT_{zz}^o - G^o C_{P_f} T_z^o = (-\Delta H)\rho r + (UA_V)^n \left(\frac{A_v^o}{A_v^n}\right)(T^n - T^o) - (UA_V)^o (T^o - T_a) \quad (2)$$

$$C_T y_t^n + G^n y_{zz}^n - \epsilon D_f C_T y_{zz}^n = \rho r \quad (3)$$

$$C_T y_t^o - G^o y_z^o + \epsilon D_f C_T y_{zz}^o = \rho r;$$

$$\rho r = \frac{A e^{E/RT^n} y^n C_{T_0}^n}{(1 + K y^n C_{T0})^2} \quad (4)$$

where G is the molar velocity (gmole/cm^{2}s), which is assumed to be constant due to the high dilution of the reactants, y is the mole-fraction of the limiting reactant, C_{pf} is the molar fluid heat capacity, while, for the other parameters, we use conventional notation. The equations are written for flow in the positive direction in the inner tube and countercurrent flow in the outside tube. Flow can be reversed by changing the sign of G. The mass-flow rate is conserved, that is, the mass-velocity should obey $G^o A_v^o = G^n A_v^n$. Note that, with infinite U^n, $T^\circ = T^n$ and we can add the two balances to find a model that is identical to that of a reactor with fast-switching flow-reversal. The catalytic domain is bound, on both sides, by inert packed-bed domains, each of length L_i. The same equations apply for the inert zones ($-L_i < z < 0$, $L < z < L + L_i$) with $r = 0$.

Continuity equations apply at the inert-catalyst borders and the Danckwerts' boundary conditions are applied at either

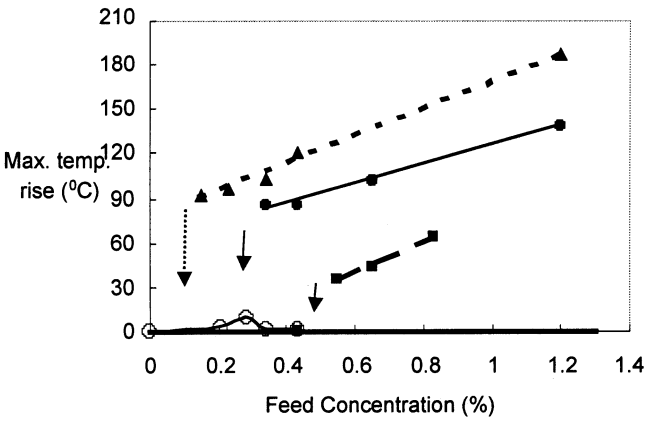

Figure 10. Comparison of maximal temperature rise as a function of feed concentration in the once-through operation, flow reversal mode, and inner recirculation mode for feed flow rate of 0.5 L/min (see Figure 8).

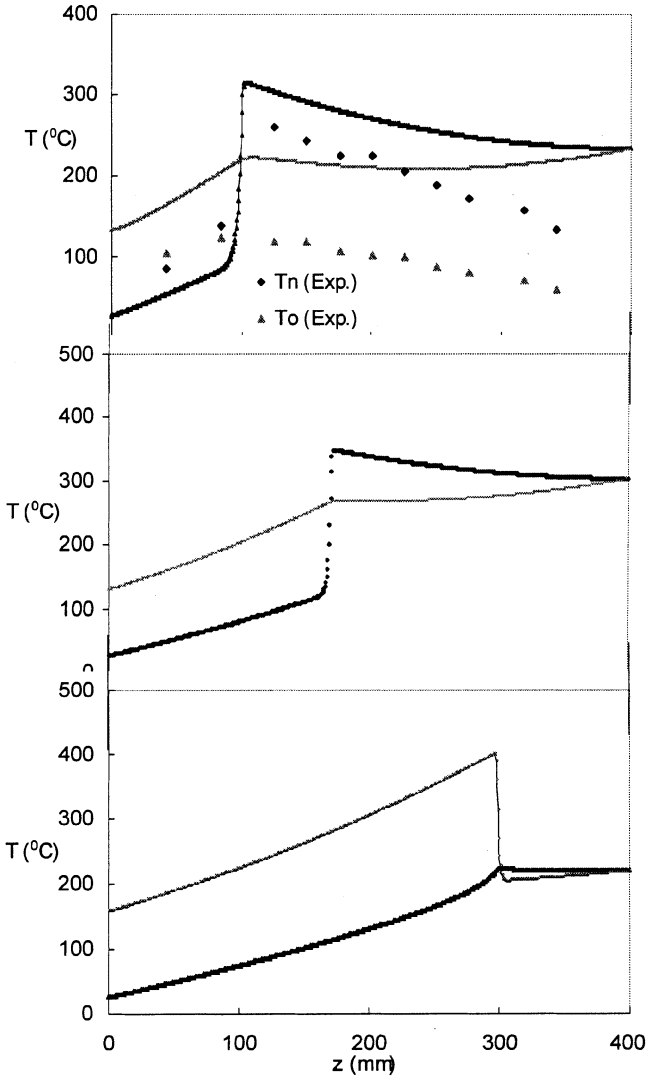

Figure 11. Simulated temperature profiles for an internal recirculation mode with 0.5% ethylene in feed at flow rates of: (a) 5.7, (b) 10, and (c) 40 L/min (flow through the inner tube). (a) denotes also the corresponding experimental temperature profiles.

edge; the left and right port of the inner and outer tubes obey:

$$(l1)\ kT_z^n|_{z=-Li} = GC_{p_f}(T^n|_{z=-Li} - T_{in})$$

$$(l2)\ \epsilon D_f C_T y_z^n|_{z=-Li} = G(y^n|_{z=-Li} - y_{in})$$

$$(r1)\ kt_z^n|_{z=L+Li} = 0$$

$$(r2)\ y_z^n|_{z=L+Li} = 0$$

$$(l3)\ kT_z^o|_{z=-Li} = GC_{p_f}(T^o|_{z=-Li} - T_{in})$$

$$(l4)\ \epsilon D_f C_T y_z^0|_{z=-Li} = G(y^o|_{z=-Li} - y_{in})$$

$$(r3)\ kT_z^0|_{z=L+Li} = 0$$

$$(r4)\ y_z^o|_{z=L+Li} = 0 \qquad (5)$$

for flow entering and leaving the inner (l1-2,r1-2) or the outer (l3-4, r3-4) tubes.

The reaction rate expression (Eq. 4) is based on an earlier study of ethylene oxidation over Pt/Al_2O_3 (Mandler et al., 1983), which was modified somewhat (Ben-Tullilah et al., 2003); the preexponential factor was calibrated by matching the simulations with experimental results in a once-through fixed-bed reactor.

The equations above take the following dimensionless form

$$Le^*\theta_\tau^n - \frac{1}{2\cdot\Gamma^n}\theta_{\xi\xi}^n + \theta_\xi^n = Da\cdot B\frac{(1-f^n)^{e^{-\frac{\gamma}{\theta n}}}}{[1+K^*(1-f^n)]^2} - \alpha_T^n(\theta^n-\theta^o) \quad (6a)$$

$$Le^*\theta_\tau^o - \frac{1}{2\cdot\Gamma^o}\theta_{\xi\xi}^o - \theta_\xi^0 = Da\cdot B\frac{(1-f^o)^{e^{-\frac{\gamma}{\theta^o}}}}{[1+K^*(1-f^o)]^2} + \alpha_T^{no}(\theta^n-\theta^o) - \alpha_T^o(\theta^o-\theta_a) \quad (6b)$$

$$f_\tau^n + f_\xi^n - \frac{1}{Pe_c^n}f_{\xi\xi}^n = Da\frac{e^{-\frac{\gamma}{\theta^n}}(1-f^n)}{[1+K^*(1-f^n)]^2} \quad (6c)$$

$$f_\tau^o - f_\xi^o - \frac{1}{Pe_c^o}f_{\xi\xi}^o = Da\frac{e^{-\frac{\gamma}{\theta^o}}(1+f^o)}{[1+K^*(1-f^o)]^2} \quad (6d)$$

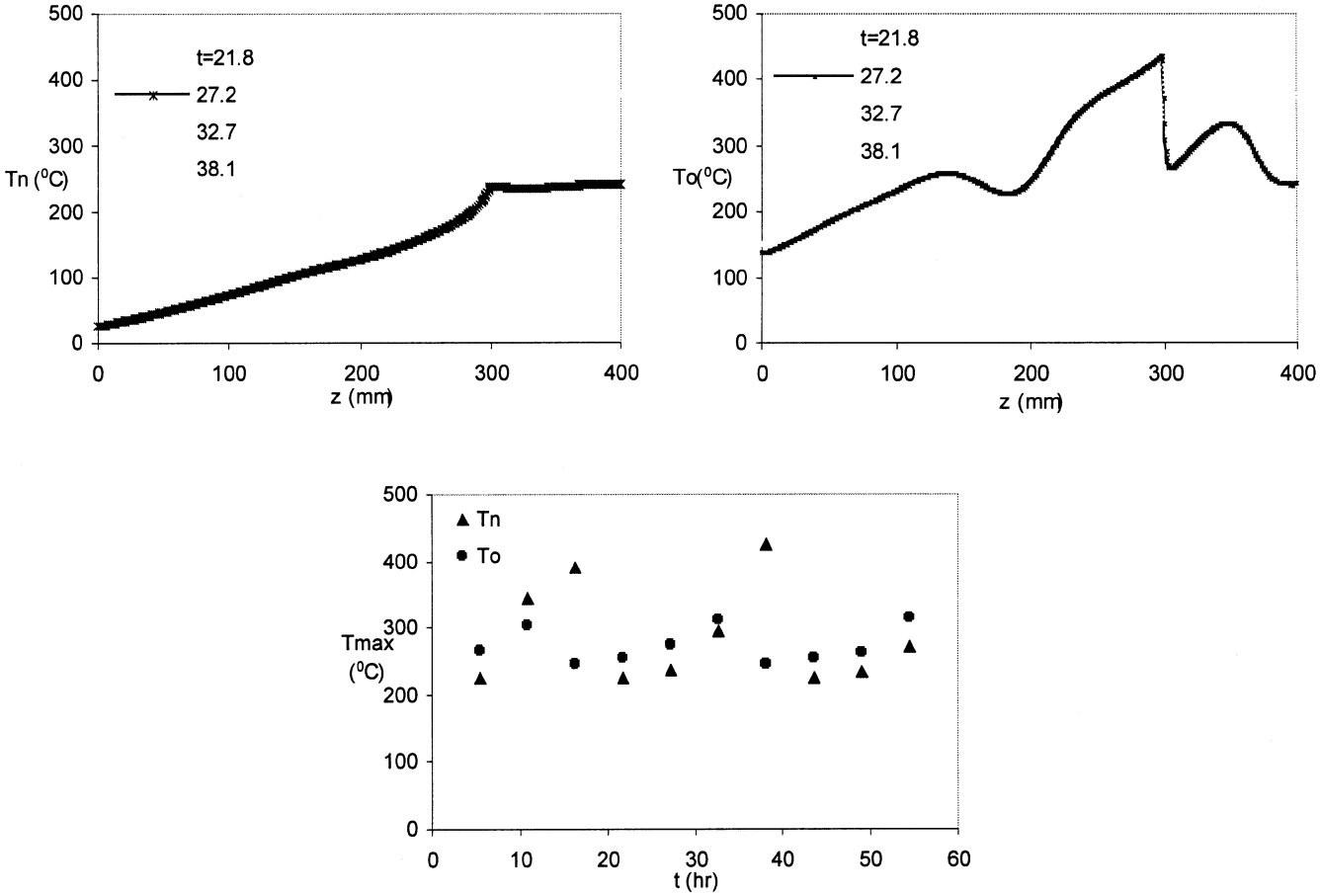

Figure 12. Dynamic pattern simulated for the inner recirculation mode for flow rate of 30 L/min, showing the axial temperatures of (a) inner and (b) outer tubes at various times, and (c) temporal dependence of the maximal temperature of inner and outer tubes.

$$(l1)\ \theta_\xi^n|_{\xi=-1} = 2\cdot\Gamma\left(\theta^n|_{\xi=-1} - \theta_{in}\right)$$

$$(l2)\ f_\xi^n|_{\xi=-1} = Pe_c^n\left(f^n|_{\xi=-1} - f_{in}\right)$$

$$(r1)\ \theta_\xi^n|_{\xi=\xi^*} = 0$$

$$(r2)\ f_\xi^n|_{\xi=\xi^*} = 0 \qquad (6e)$$

The dimensionless parameters and variables are defined in a conventional way (see notation).

Typical temperature profiles in the internal-recirculation mode (Figure 11) exhibit a sharp front at the entrance to the catalytic section, at low flow rates, or a front positioned somewhere inside the reactor (Figure 11b), at intermediate flows, or an oscillatory dynamic in which the front travels outside the inner catalytic domain and into the outer one and back again at higher flow rates. The dependences of maximal temperature and of front position on the flow rate plotted in Figure 13, showing that the front is located at the entrance for a flow rate lower than 7 L/min, but at higher flow rates, its position shifts, while the maximal temperature increases, until it reaches the end of the catalytic zone of a flow rate of 30 L/min. At higher flow rates, the front shifts to the outer tube (Figure 11c). The temporal solution of the oscillatory behavior that develops for 30 L/min. is portrayed in Figure 12 showing a very long period ($\sim$ 22 h).

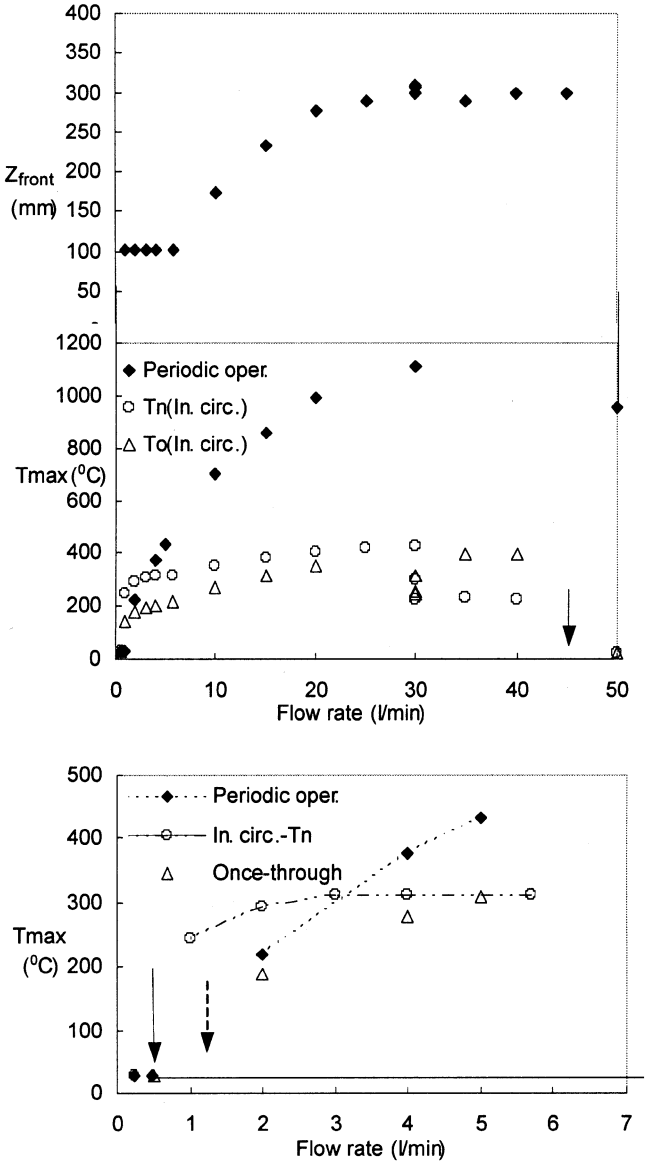

Figure 13. Maximal temperatures as a function of flow rate and extinction points simulated for flow reversal, internal recirculation and once-through modes in the experimental (nonadiabatic) reactor for two ranges of the flow rate: (a) dependence of the front position on the flow rate for the recirculation modes; (b) 0–50; (c) 0–7.

These results are compared with one set of experimental results in Figure 11(a), both showing a steep front at the entrance to the reactor, but the agreement could be improved by better matching the various heat-transfer coefficients of the problem (see also Ben-Tullilah et al., 2003). While it is evident that the heat-transfer coefficients should be higher than those employed in the simulations, initial attempts to use lower values led to the extinction of the whole reactor. That will require reassessment of the kinetic parameters, which is beyond the scope of this work.

The problem of parameter estimation is emphasized again in Figure 14 which simulates the behavior shown in Figure 3: Simulations using the parameters employed for Figures 11–13 led to an extinguished state. The profiles shown in Figure 14, using preexponential factor (A) that is twice that used earlier, produced an ignited state, but, with increasing flow rate, the front shifts downstream, as opposed to experimental results (Figure 3) in which the front is always located at the inert-catalyst boundary. Even though the simulations predict qualitatively poor agreement with the experimental results, the prediction of the maximal temperature is quite adequate (Figure 4).

We compare now four modes of operation (Figure 13), for the conditions of this study with significant heat losses: the

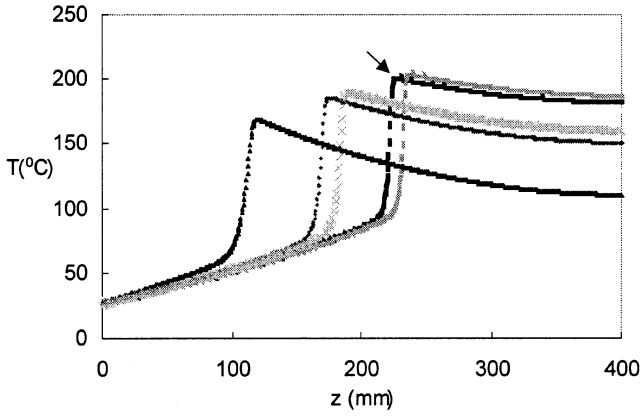

Figure 14. Simulated axial temperature profiles for inner recirculation mode with various flow rates for ethylene feed concentration of 0.25%.

Compare with Figure 3.

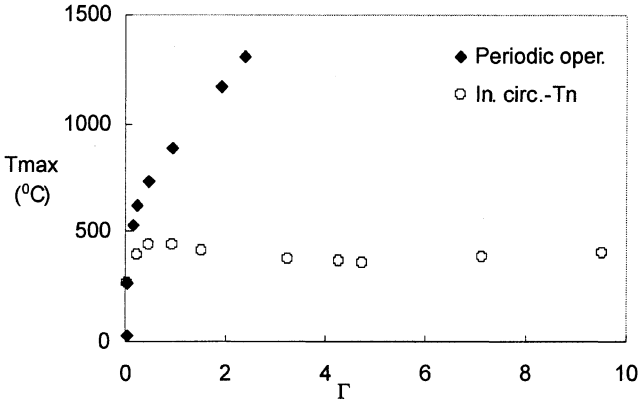

Figure 15. Maximal temperature as a function of reduced flow rate (Γ) simulated for reverse flow and internal recirculation modes in an adiabatic reactor.

flow reversal reactor, the internal recirculation reactor with feeding to the inner tube, and the once through reactor. The flow reversal reactor is simulated here for the full reactor volume that incorporates both inner and outer tubes (Ben-Tullilah et al., 2003). We compare the maximal temperature and the extinction points at high or low flow rates. The comparison shows that, at high flow rates, the flow-reversal reactor yields higher maximal temperatures than the internal recirculation reactor. The former does not extinct at high flow rates (at least not for flow rates lower than 150 L/min), while the latter undergoes extinction at about 45 L/min. The extinction points, upon decreasing flow rates, occur earlier in the flow reversal reactor than in the recirculation reactor. Also, for the domain that corresponds to a stationary front at the inlet to the recirculation reactor, it shows higher temperatures than the flow-reversal reactor. Comparison of the internal recirculation mode with the once-through operation shows that extinction of the latter occurs at an earlier point on both sides of the flow-rate domain.

Comparison of flow reversal and internal recirculation operation in an *adiabatic* reactor shows similar maximal temperatures at low flow rates, but, at high flow rates, the latter mode reaches an asymptotic temperature that depends on the U, while the former continues to climb linearly with flow rate (Figure 15).

The difference between the experimental and simulated temperature is attributed to several factors: recall that we did not try to fit the experimental data. The data of Figure 11 suggest that better fitting of the heat-transfer coefficient could be achieved. Moreover, the profile forms a front, so that matching the profile requires matching the front position. The effect of wall conductivity and heat capacity may be important. A simulation to that effect in part I of this study (Ben-Tullilah et al., 2002) demonstrates this point. However, if the effect is large, it calls for the application of a two-dimensional (2-D) model, which is beyond the scope of this work.

Conclusions

Experiments and simulations, with ethylene oxidation as a model reaction, show that, at high flow rates, the flow reversal reactor is superior to the internal recirculation reactor, as the temperature in the former increases with the feed rate, while the temperature in the latter reaches an asymptotic value (Figure 15) or starts to decline. However, the situation is reversed at low flow rates, and the extinction point encountered in the recirculation reactor occurs at lower concentrations than in the flow-reversal operation. The flow rate that marks the transition between the two depends on the internal heat-transfer coefficients and implementation of this operation, which is simpler technically, calls for finding ways to improve the internal heat transfer.

Simulations revealed also the existence of solutions with stationary fronts or oscillatory fronts in which the front travels through part of the system. These results are surprising, as simple kinetics were employed here, but they join a growing class of dynamic behavior in flow reactors with recycle or feedback.

In a future publication we will derive an approximate solution for a reactor with internal recirculation: This type of operation is similar to that of two heat-exchanging reactors with countercurrent flow, and both types of operation depend on the heat-exchange coefficient. In the limit of infinitely-fast heat transfer the models of both reactors are similar to that of the flow-reversal reactor with fast switching of flow. As demonstrated in part one of this study (Ben-Tullilah et al., 2002), the studied reaction is self-inhibited and highly-exothermic. Such kinetics are characterized by a steep temperature dependence and, for high temperatures, the reaction rate can be assumed to be instantaneous or very fast. We can apply this fast-reaction assumption in order to derive approximate solutions and study the effect of feed flow rates and heat loss. This approach is supported by the results at high flow rates (Figure 3) and some of the results at low flow rates (Figures 7 and 8), which demonstrates that the reaction commences at the inert-catalyst boundary; yet, certain low flow-rates results (Figure 6) do not support this approach.

Acknowledgment

Work supported by the U.S.-Israel Binational Science Foundation.

Notation

A = pre-exponentional reaction rate constant, $7.8 \cdot 10^{10} s^{-1}$
A_V^n = specific surface area of the inner tube, 140 m^{-1}
A_v^o = specific surface area of the outer tube, 133.4 m^{-1}
B = dimensionless temperature rise, $((-\Delta H)y_{in}/C_{pf}T_{in})$
C_T = total concentration, 40.92 gmole/m^3
C_{peff} = effective heat capacity, $((1-\epsilon)\rho C_{p_s} + \epsilon C_T C_{pf})$, J/grK
C_{pf} = molar gas heat capacity, 28.84 J/gmole·K
C_{ps} = solid heat capacity, 0.74 J/gr·K
D_a = Damköhler number, (AC_TLi/G)
D_f = dispersion coefficient, 1.14* 10^{-4} m^2/s
E = Activation energy, $2.23 \cdot 10^4$ kJ/kmol
f = conversion, $(1 - C/C_{in} = 1 - y/y_{in})$
G = molar velocity, gmole/m^2s
k = solid thermal conductivity, 1.18 J/m·s·K
K = adsorption coefficient, 0.257m^3/gmole
K^* = dimensionless adsorption coefficient, $(KC_T y_{in})$
L = catalytic zone length, 0.2 m
Li = inert zone length, 0.1 m
Le^* = Lewis number, $(\rho C_{peff}/C_T C_{pf})$
Pe_c = Peclet number for mass, $(GL_i/\epsilon D_f C_{in})$
r = reaction rate
t = time, s
T = temperature, K
T_a = ambient temperature, 298 K

T_m = maximal temperature, K
U^n = heat-transfer coefficient of the inner tube correlated for flow rate, $(0.674.(G/C_T)+3.8465)$ J/m$^2\cdot$s$\cdot$K
U^o = heat transfer coefficient of the outer tube correlated for flow rate, $(0.123.(G/C_T)+0.7005)$ J/m$^2\cdot$s$\cdot$K
y = mole fraction of the limiting reactant, C/C_T
z = axial coordinate, m

Greek letters

ΔH = heat of combustion, $1.32\cdot10^6$ J/kmol
α_T^n = dimensionless heat transfer coefficient for the inner tube
α_T^{no} = dimensionless heat transfer coefficient between the tubes
α_T^o = dimensionless heat transfer coefficient for the outer tube
ϵ = void fraction, 0.4
Γ = reduced flow rate, $(GC_{pf}L_i/2k)$
γ = dimensionless activation energy, (E/RgT_{in})
θ = dimensionless temperature, (T/T_{in})
ρ = solid density, $1.588\cdot10^6$ g/m^3
τ = dimensionless time, $(t^*G/C_{\text{in}}L_i)$
ξ = dimensionless axial coordinate, (z/L_i)
$\xi*$ = dimensionless modulus $((L+L_i)/L_i)$
$-\Delta T_{ad}$ = adiabatic temperature rise, K

Superscript

c, i = catalytic or inert zone
n, o = inner or outer tube

Subscript

a = ambient
eff = effective
ent = entrance
f = fluid
in = Inlet

Literature Cited

Ben-Tullilah, M., E. Alajem, R. Gal, and M. Sheintuch, "Flow Rate Effects in Flow-Reversal Reactors: Experiments, Simulations and Approximations," *Chem. Eng. Sci.*, **58**, 1135 (2003).

Bhatia, S. K., "Analysis of Catalytic Reactor Operation with Periodic Flow Reversal," *Chem. Eng. Sci.*, **46**(1), 361 (1991).

Boreskov, G. K., and Y. Sh. Matros, "Unsteady-State Performance of Heterogeneous Catalytic Reactions," *Catal. Rev. - Sci. Eng.*, **25**, 551 (1983).

Boreskov, G. K., Yu. Sh. Matros, and O. V. Kiselev, "Catalytic Processes under Nonsteady-State Conditions. I. Thermal Front in the Immobile Catalyst Layer," *Kinet. Katal.*, **20**(3), 773 (1979).

Burghardt, A., M. Berezowski, and E. W. Jacobsen, "Approximate Characteristics of a Moving Temperature Front in a Fixed-Bed Catalytic Reactor," *Chem. Eng. Process.*, **38**, 19 (1999).

Eigenberger, G., and U. Nieken, "Catalytic Combustion with Periodic Flow Reversal" *Chem. Eng. Sci.*, **43**, 2109 (1988).

Froment, G. F., and K. B. Bischoff, *Chemical Reactor Analysis and Design*, (2nd ed.), Wiley, New York (1990).

Gawdzik, A., and L. Rakowski, "Dynamic Properties of the Adiabatic Tubular Reactor with Switch Flow," *Chem. Eng. Sci.*, **43**, 3023 (1988).

Harmsen, J. M. A., J. H. B. J. Hoebink, and J. C. Schouten, "Transient Kinetic Modeling of the Ethylene and Carbon Monoxide Oxidation over a Commercial Automotive Exhaust Gas Catalyst," *Ind. Eng. Chem. Res.*, **39**, 599 (2000).

Lauschke, G. and Gilles, E. D., "Circulating Reaction Zone in a Packed Bed Loop Reactor," *Chem. Eng. Sci.*, **49**(24B), 5359 (1994).

Mandler, J., R. Lavie, and M. Sheintuch, "An Automated Catalytic System for the Sequential Optimal Discrimination between Rival Models," *Chem. Eng. Sci.*, **38**, 979 (1983).

Matros, Yu. Sh., *Studies in Surface Science and Catalysis (43): Catalytic Processes Under Unsteady-State Conditions*, Elsevier, Amsterdam (1989).

Matros Yu. Sh., A. S. Noskov, and V. A. Chumachenco, "Progress in Reverse-Process Application to Catalytic Incineration Problems," *Chem. Eng. Prog.*, **32**, 89 (1993).

Matros, Yu. Sh., and G. A. Bunimovich, "Reverse-Flow Operation in Fixed Bed Catalytic Reactors," *Catal. Rev.-Sci. Eng.*, **38**, 1 (1996).

Nieken, U., K. Gregorios, and G. Eigenberger, "Control of the Ignited Steady State in Autothermal Fixed-Bed Reactors for Catalytic Combustion," *Chem. Eng. Sci.*, **49**, 5507 (1994).

Rehacek, J., M. Kubicek, and M. Marek, "Periodic, Quasiperiodic and Caotic Spatitemporal Patterns in a Tubular Catalytic Reactor with Periodic Flow Reversal," *Comput. Chem. Eng.*, **22**, 283 (1998).

Thullie, J. and A. Burghardt, "Application of the Flow Reversal Reactor to the Methanol Synthesis," *Unsteady State Processes in Catalysis*, ed., Yu. Sh. Matros, VNU Science Press, Utrecht-Tokyo, pp. 687-692 (1990).

Van de Beld, B., R. A. Borman, O. R. Derkx, B. A. A. van Woezik, and K. R. Westerterp, "Removal of Volatile Organic Compounds from Polluted Air in a Reverse Flow Reactor: An Experimental Study," *Ind. Eng. Chem. Res.*, **33**, 2946 (1994).

Van de Beld, B., and K. P. Westerterp, "Air Purification by Catalytic Oxidation in a Reactor with Periodic Flow Reversal," *Chem. Eng. Technol.*, **17**, 217 (1994).

Manuscript received Apr. 26, 2002, revision received Oct. 9, 2002, and final revision received Mar. 17, 2003.